Socioeconomic disparities in heat exposure in India: A mobility-based analysis

Citation for the original published paper (version of record):
Ma, J., Sun, C., Gabilondo, S. et al (2026). Socioeconomic disparities in heat exposure in India: A mobility-based analysis. Sustainable Cities and Society, 145.
http://dx.doi.org/10.1016/j.scs.2026.107437

(article starts on next page)

Sustainable Cities and Society 145 (2026) 107437

Contents lists available at ScienceDirect

Sustainable Cities and Society

journal homepage: www.elsevier.com/locate/scs

Socioeconomic disparities in heat exposure in India: A mobility-based analysis☆

Jue Ma [a], Chenchen Sun [a,*], Santiago Garcia Gabilondo [a], Carl Torbjörnsson [b], Qiang Guo [c], Yuya Shibuya [d], Yoshihide Sekimoto [a]

[a] Center for Spatial Information Science, The University of Tokyo, Tokyo, Japan
[b] Department of Computer Science and Engineering, Chalmers University of Technology, Gothenburg, Sweden
[c] Institute of Systems and Information Engineering, University of Tsukuba, Ibaraki, Japan
[d] Interfaculty Initiative in Information Studies, The University of Tokyo, Tokyo, Japan

ARTICLE INFO

Dataset link: https://cds.climate.copernicus.eu/datasets/reanalysis-era5-land, https://dataforgood.facebook.com/dfg/tools/relative-wealth-index, https://dhsprogram.com

Keywords:
Heat exposure
Heat stress
Human mobility
Socioeconomic disparities
Public health

ABSTRACT

Heat exposure is an escalating public health concern, where limited policy attention and infrastructure constraints hinder effective risk assessment and response. This study introduce a multi-perspective and multi-scale analytical framework to quantify socioeconomic disparities in heat exposure using spatiotemporally resolved data, providing key insights for targeted public health interventions and policy development. Taking India as the study area, we integrated temperature, human mobility, and socioeconomic data at geohash-5 level and 3-hour intervals throughout 2019. Our results reveal distinct spatial–temporal patterns of extreme heat, suggesting that socioeconomic conditions are weakly associated with differences in heat exposure, particularly across populated metropolitan regions. A significant but modest association between the Relative Wealth Index (RWI) and Wet Bulb Globe Temperature (WBGT) is observed at the metropolitan scale ($r \approx 0.32$***), reflecting broad population scale gradients across large urban regions, rather than neighborhood level intra-urban variability. Mobility analysis further shows that lower-income groups not only experience greater heat stress during daily activities but also face constrained capacity to adapt their travel behavior under extreme heat. These findings underscore the need to incorporate mobility-informed exposure assessments. The proposed framework offers practical guidance for data-driven, equity-oriented planning and is particularly suited for developing country contexts where high-quality big data remains limited.

1. Introduction

With global warming and rapid urbanization, the frequency and intensity of extreme heat events are increasing worldwide (Guo, Mistry et al., 2024; Klingelhöfer et al., 2023), posing serious threats to public health, including heat-related illnesses such as heat stroke (Guo, Yuan et al., 2024; Hess et al., 2023; Kim et al., 2016). Consequently, heat exposure has gained significant research attention as a critical environmental risk, especially within urban contexts.

In recent years, studies have extensively explored how extreme weather events influence human mobility patterns within urban areas (Chapman et al., 2017; Zhang et al., 2019). These studies show significant disruption in human mobility in response to events such as hurricanes, wildfire smoke (Hatchett et al., 2021), rainstorms, and snowstorms (Zhang et al., 2019). Moreover, growing evidence has demonstrated strong correlations between extreme temperatures and urban mobility patterns. For instance, Gu et al. (2024) utilizing mobile application data, revealed that extreme heat inhibits people flow toward city centers and promotes movement toward suburbs, influencing short-distance travel behaviors.

However, existing studies primarily focus on developed regions with abundant data resources and well-established infrastructure, often emphasizing specific vulnerable populations (Basu & Samet, 2002; Kovats & Hajat, 2008; Yin et al., 2021), and occupational heat stress (Gubernot et al., 2014; Jay & Kenny, 2010; Spector et al., 2019). Additionally, research on chronic climate impacts has largely examined spatiotemporal patterns of heat exposure (Kyaw et al., 2023; Liu et al., 2024) and

☆ This article is part of a Special issue entitled: ‘Environmental Extremes’ published in Sustainable Cities and Society.

* Correspondence to: Ce509, 4-6-1, Komaba, Meguro-ku, Tokyo 153-8505, Japan.
E-mail addresses: majue@csis.u-tokyo.ac.jp (J. Ma), sun_chenchen@csis.u-tokyo.ac.jp (C. Sun), garcia-s@csis.u-tokyo.ac.jp (S.G. Gabilondo), carltor@chalmers.se (C. Torbjörnsson), qiangguo@kz.tsukuba.ac.jp (Q. Guo), yuya-shibuya@iii.u-tokyo.ac.jp (Y. Shibuya), sekimoto@csis.u-tokyo.ac.jp (Y. Sekimoto).

https://doi.org/10.1016/j.scs.2026.107437
Received 31 March 2025; Received in revised form 23 April 2026; Accepted 24 April 2026
Available online 7 May 2026

urban heat island effects (Jacobs et al., 2019; Liu et al., 2024). Few have explored socioeconomic disparities, especially from a mobility perspective.

Critical knowledge gaps remain in understanding of heat exposure risks and their implications in developing countries, particularly in regions of the Global South. These areas not only face existing hot and humid climates but are projected to experience more severe increases in extreme heat under climate change scenarios (Mora et al., 2017; Suter et al., 2019). The climate crisis is inherently inequitable, disproportionately impacting impoverished populations who contribute least to greenhouse gas emissions (Campbell-Lendrum & Corvalán, 2007). Furthermore, developing countries often face structural challenges such as weak healthcare systems and inadequate infrastructure deficiencies due to their economic constraints. A significant portion of low-income populations live in informal settlements, where protective measures against extreme climate are severely limited. Despite these potential vulnerabilities, research addressing heat exposure and mitigation strategies in low- and middle-income countries remains limited (Hondula et al., 2017; Kjellstrom et al., 2009), particularly with respect to human mobility, which significantly influences actual exposure levels.

To bridge these research gaps, our study proposes a multi-perspective and multi-scale analytical framework to assess socioeconomic disparities in heat exposure, incorporating environmental, mobility, and socioeconomic data. Specifically, we address the following research questions:

- What are the spatiotemporal patterns of heat exposure experienced by residents across India, especially in urban contexts?
- Do populations from different socioeconomic groups experience unequal levels of heat exposure risk under similar climatic conditions?
- How do these disparities manifest from static (residence-based), semi-static (activity-based), and dynamic (trip-based) perspectives?

We employ India as our case study, as it represents a critical context with its high population density, pronounced socioeconomic inequality, widespread informal housing conditions, and predominantly tropical and subtropical climate characterized by high temperature and high humidity. Additionally, the country's diverse socioeconomic landscape, coupled with limited cooling infrastructure, provides a meaningful opportunity to examine how socioeconomic status influences heat exposure disparities.

In this study, we define structural inequalities as spatially embedded disparities in access to infrastructure, urban amenities, and mobility resources, which shape individuals' exposure to environmental risks and constrain their capacity to respond (Hsu et al., 2021). For example, in the context of heat exposure, lower-income groups may have less access to green spaces, air-conditioned environments, or efficient public transportation—factors that directly influence their ability to avoid or mitigate heat stress (Laue et al., 2022).

Specifically, we utilize high-resolution spatiotemporal data integrating human mobility patterns and socioeconomic indicators to investigate how different socioeconomic groups in Indian cities experience and mitigate heat exposure, providing crucial insights for targeted public health interventions and policy development.

2. Literature review

2.1. Necessity of heat exposure study in India

The intensification of extreme heat due to anthropogenic climate change poses a severe global challenge. Multi-scale analyses of the 2021 Western U.S. heatwaves showed that large-scale synoptic highs, mesoscale circulations, and local urban heat island (UHI) effects interacted to create temperature anomalies exceeding 10–20°C above climatological norms, underscoring the compound nature of urban heat risks (Chen et al., 2023). Similar trends are evident across the Global South. In India, the frequency and intensity of heat waves (HW) and severe heat waves (SHW) have increased markedly since the mid-20th century, with higher mortality risks in coastal regions (Singh et al., 2021). Moreover, urbanization exacerbates exposure through declining vegetation and increasing impervious surfaces. In India's National Capital Region, land surface temperature (LST) rose by 2.7°C between 2005 and 2020, expanding the UHI footprint and degrading ecological conditions (Mandvikar et al., 2024). And a J-shaped temperature-mortality curve, with mortality rates rising sharply when temperatures exceeded 35 degrees has been found in Ahmedabad (Sharma et al., 2024). Such evidence highlights the link between urban planning, climate adaptation, and public health. As high heat correlates with elevated mortality, productivity loss, and migration pressures, particularly in rapidly growing Indian cities, understanding heat exposure is crucial for sustainable urban resilience.

2.2. Progress in global heat exposure studies

Research on heat exposure in the field of urban planning has proliferated across multiple countries these years. Early work in the U.S. and Europe focused on census-based vulnerability mapping (Aubrecht & Özceylan, 2013; Hsu et al., 2021), while more recent analyses extend to the Global South, China, India, and the Middle East, where rapid urbanization interacts with climate change to create new hotspots of risk. For example, Wang et al. (2024) assessed extreme heat exposure in 320 Chinese cities using a Hazard Exposure Vulnerability framework, revealing that over 97% of cities experienced worsening exposure trends from 2000 to 2020. Similarly, Zou et al. (2025) examined 301 Chinese cities and found population weighted exposure rising consistently over two decades, driven by dense built-up expansion and limited adaptive infrastructure. Li, Yigitcanlar et al. (2024) developed a Comprehensive Heat Vulnerability Index (CHVI) in Australia by incorporating socio-demographic and health indicators, finding that vulnerability decreases from urban to rural areas, yet inequity remains pronounced in city centers. Similarly, Kitchley et al. (2024) proposed a contextual vulnerability framework for Madurai, India, integrating social capital and cultural values alongside meteorological and biophysical parameters to reveal socially marginalized zones. These multi-criteria indices demonstrate how heat exposure interacts with socio-economic and infrastructural disparities in diverse urban contexts.

Methodologically, the field has evolved from static, homogeneous temperature analyses toward dynamic frameworks that focus on internal variations and integrate multiple data sources. For example, El Kenawy et al. (2024) used regression-based LST trends to analyze day-night heat stress across Middle Eastern cities, revealing stronger night-time warming inland and millions at risk under sustained heat exposure. Zou et al. (2025) introduced population-weighted heat exposure (PWE) metrics to capture urban–rural disparities across 301 Chinese cities, emphasizing the role of human distribution in shaping exposure patterns. The growing use of high-resolution satellite data (e.g., ECOSTRESS, Landsat) has enabled socio-spatial comparisons of heat exposure by income level. For instance, Raj et al. (2025) contrasted Seoul and London, finding that low-income neighborhoods in London suffer greater heat intensities due to uneven greenspace distribution, whereas Seoul exhibits more equitable thermal conditions because of compact housing patterns and balanced urban planning. Furthermore, Lyu et al. (2024) used location-based social media and natural language processing to map human perceptions of heat exposure in real time, demonstrating how participatory data can complement remote sensing for urban heat resilience. Most recently, Wu et al. (2025) integrated mobile phone signaling data with mean radiant temperature (MRT) maps to distinguish residence-based and mobility-based exposure, addressing the Neighborhood Effect Averaging Problem (NEAP). Their results from Chongqing show that daily mobility significantly moderates exposure extremes, producing upward averaging in urban cores and downward averaging in suburban zones, marking a paradigm shift from static spatial exposure mapping toward mobility-aware approaches. Collectively, these studies highlight the complexity of urban heat exposure as an intersectional and multi-scalar problem linking climate science, public health, and urban planning. The growing body of work from both the Global North and South underscores that addressing heat inequality requires not only technological mitigation but also social and spatial justice.

2.3. Persistent gaps and summary

Despite the progress, significant gaps still remain in understanding and addressing heat exposure inequality. (1) Static exposure assumptions. Most existing studies define exposure based on residential or census tracts, neglecting individuals traverse diverse thermal environments. As Wu et al. (2025) show, ignoring mobility systematically biases exposure estimates, particularly for outdoor workers and commuters which are common in the Global South. (2) Underrepresentation of the Global South. While equity has been well documented in North American and European contexts (Hsu et al., 2021), few studies integrate social inequity with dynamic mobility in cities such as Delhi, Lagos, or São Paulo. Yet, evidence from India's NCR (Mandvikar et al., 2024) and Chinese metropolitan regions (Wang et al., 2024; Zou et al., 2025) reveals rapid urban expansion coupled with inadequate adaptive capacity. The Global South's deficit in both quantity and quality of green infrastructure further widens the thermal inequality gap (Li, Svenning et al., 2024). (3) Temporal and behavioral granularity. Heat exposure fluctuates by hour, season, and activity type, but diurnal and behavioral dimensions are rarely captured. Studies in the Middle East and East Asia (El Kenawy et al., 2024; Ming et al., 2024) demonstrate significant day–night and subgroup variations, yet large-scale, time-resolved assessments remain scarce.

By integrating static environmental layers with dynamic human trajectories, experienced rather than merely residential heat exposure can be reconstructed. This approach enhances realism by capturing how people clustering, traveling in the city space shape actual thermal stress. It further enables equity analysis, revealing whether low-income or marginalized groups endure higher exposure and choose different travel patterns when facing heat challenge. The findings of temporal variations help us to identify critical intervention periods, such as shading for peak-hour transit routes or nighttime cooling in dense urban cores.

In summary, heat exposure research has evolved from climatic mapping to complex socio-environmental analysis, yet most studies remain spatially static and demographically coarse. Incorporating mobility transforms the understanding of exposure from where people live to where and when they move, unveiling the hidden inequalities of daily urban life. For Global South cities, where exposure, vulnerability, and mobility intersect sharply, such multi-scale, mobility-based approaches can redefine heat-resilience planning by revealing "moving inequalities" in thermal risk and guiding equitable, adaptive urban design.

3. Materials and methods

3.1. Study area

This study focuses on India, a rapidly urbanizing country in South Asia with a population exceeding 1.4 billion. Administratively, India comprises 28 states and 8 union territories. Despite notable economic growth, the urbanization rate remains at approximately 35%–38%, indicating that a large majority of the population still resides in rural areas. India is highly vulnerable to extreme heat, especially during the pre-monsoon summer months, with large parts of the Indo-Gangetic Plain and central India regularly encountering temperatures exceeding 40°C. The increasing frequency and intensity of heatwaves pose a growing threat to public health and sustainable development.

To ensure the robustness of our findings and mitigate boundary sensitivity, this study employs a multi-scale analytical framework encompassing four spatial levels (Fig. 1):

1. National Scale (entire country): A baseline analysis using approximately 145,600 Geohash-5 units across all of India.
2. Populated-area Scale (areas with active users in PD dataset): A refined analysis covering approximately 20,800 Geohash-5 units wiith active user data in the Population Density dataset, excluding sparsely populated rural regions or non-urban built-up areas.
3. Metropolitan-region scale (21 cities): An urban-focused analysis of India's 21 top metropolitan cities (e.g., Mumbai, Delhi, Kolkata), geographically dispersed and representing approximately 630 Geohash-5 units.
4. Individual city scale (typical city area): Each metropolitan cities is treated as an individual study unit, enabling an exploratory analysis of coarse spatial gradients across the city's Geohash-5 units. Given the limited spatial resolution of the underlying data, this analysis does not aim to capture fine-scale or neighborhood-level intra-urban variability.

3.2. Data source

Human mobility data: We leverage anonymized, aggregated human mobility data provided by Spectus Social Impact, obtained as part of the Netmob 2024 data challenge (Zhang et al., 2024). The dataset includes high-resolution population density (PD) and origin–destination (OD) matrices aggregated at geohash-5 level (4.9 km * 4.9 km) and recorded at 3-hour intervals for the entire year of 2019 across India. All data was collected following informed consent protocols, ensuring full anonymity and ethical compliance. It enables us to assess static population distributions during periods of elevated temperatures and analyze dynamic human mobility patterns across spatial units. Preliminary analysis of PD data indicates pronounced user densities in northern and southwestern regions, which provide crucial spatial context for subsequent heat exposure analysis (Fig. 3, top-right).

Temperature data: Hourly 2 m temperature, 2 m dewpoint temperature, 10 m u-component of wind, 10 m v-component of wind, and surface solar radiation downwards data were obtained from the *ERA5-Land hourly data from 1950 to present* dataset provided by the Climate Data Store (Copernicus Climate Change Service, 2025). These variables were collected for calculation of the Wet Bulb Globe Temperature (WBGT), which would be explained in Section 3.3.1. The ERA5-Land dataset offers high-resolution meteorological data at approximately 9 km spatial resolution.

To align the temperature data spatially with the mobility dataset, we performed nearest-neighbor interpolation method to map the value onto the Geohash-5 units (with scale of 4.9 km resolution). Temporally, the hourly temperature data was further aggregated into corresponding 3-hour intervals.

Socioeconomic data: To quantify socioeconomic disparities in heat exposure, we employed the Relative Wealth Index (RWI) dataset provided by Chi et al. (2022). The RWI, derived from de-identified connectivity data, satellite imagery, and other nontraditional data sources, provides a high-resolution (2.4 km) proxy for living standards within countries. It is particularly advantageous in low- and middle-income settings with limited traditional economic indicators. The RWI has been externally validated by Chi et al. (2022) against Demographic and Health Surveys (DHS) wealth quintiles, showing strong correlations ($r > 0.8$) across multiple LMICs, including India. Furthermore, a comparative analysis of wealth index predictions in Africa shows that the RWI method yields the closest estimates to ground-truth data (Karsai et al., 2024).

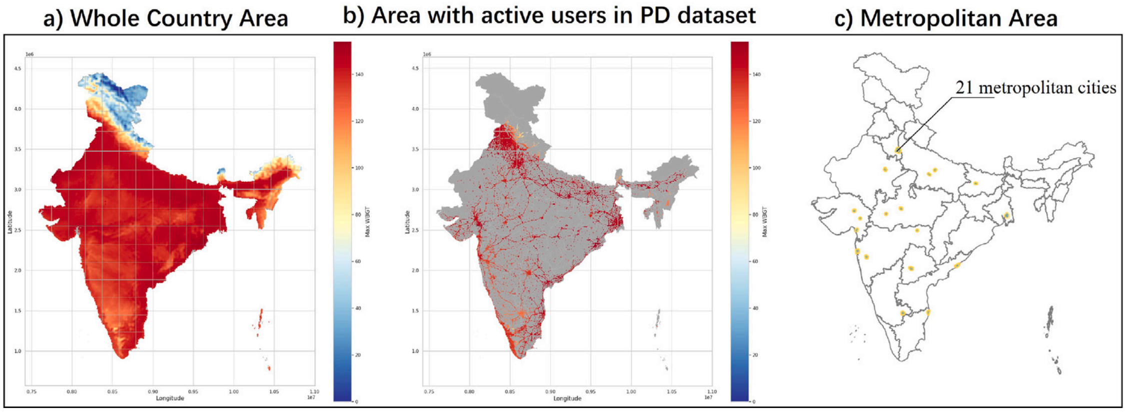

Fig. 1. Study area definition.

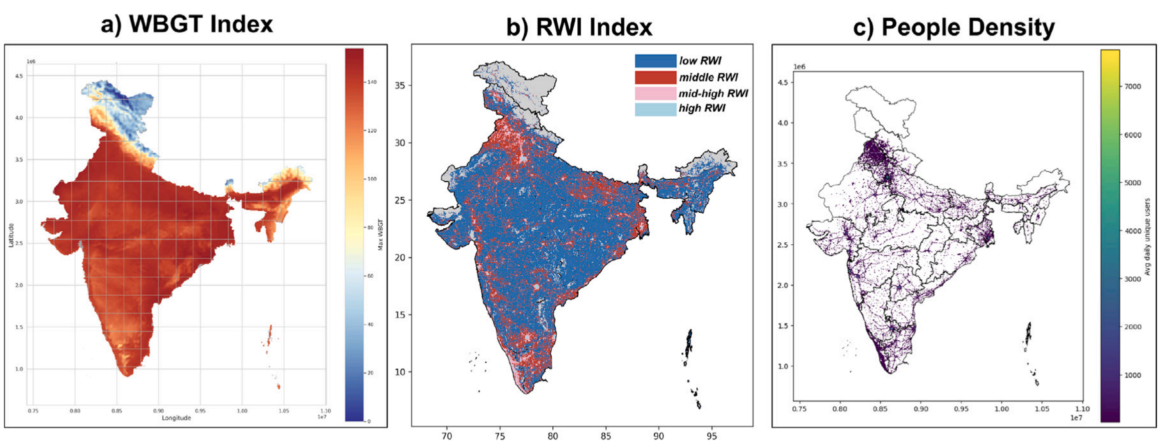

Fig. 2. Three types of data sources.

Given the lack of detailed socioeconomic information in our mobility data, the RWI dataset captures spatial relative wealth distributions. Considering users' uneven spatial distribution and possible sampling bias in mobility data, it is appropriate to use quartiles to divide users identified from the mobility dataset into four equal-sized groups of varying economic levels. We categorize the continuous RWI value into four socioeconomic groups: low RWI ($\leq$0.68), middle RWI (0.68 $<$ RWI $\leq$ 0.97), mid-high RWI (0.97 $<$ RWI $\leq$ 1.16), and high RWI ($\geq$1.16). This classification is particularly relevant in India's context, where disparities in infrastructure significantly influence vulnerability to heat stress. The resulting spatial RWI distribution (Fig. 2, middle) highlights the substantial wealth disparities across India, where most regions exhibit low RWI, while mid-high and high RWI groups are concentrated in some urban centers, reinforcing the importance of integrating socioeconomic factors into heat exposure assessments.

3.3. Methods

Combining these mobility, meteorological, and socioeconomic datasets, our study establishes a methodological framework (Fig. 3) to quantify socioeconomic disparities in heat exposure across diverse spatial–temporal scales in India.

3.3.1. Overall heat exposure of the population

Heat stress is measured using the Wet Bulb Globe Temperature (WBGT), one of the most widely used indices for assessing heat exposure that considers temperature, humidity, solar radiation, and wind effects (Li et al., 2020):

$$\mathrm{WBGT} = 0.7T_{nw} + 0.2T_g + 0.1T_a \tag{1}$$

where T_a represents the dry bulb temperature, T_{nw} the natural wet bulb temperature in the natural environment of wind and sun, and T_g the globe temperature, estimated based on solar shortwave radiation and the terrestrial longwave radiation obtained from ERA5-Land data.

We calculate the WBGT values at 3-hour intervals throughout the year 2019 and assigned to each spatial unit in our study area, using the Liljegren method (Lemke & Kjellstrom, 2012). To evaluate heat stress level, we adopt the hazard ranking for outdoor heat stress levels of daily living proposed by the Japanese Society of Biometeorology (Kikumoto et al., 2016). This ranking categorizes WBGT levels into five risk levels: Danger (WBGT $\geq$ 31.0), Severe warning (28.0 $<$ WBGT $\leq$ 31.0), Warning (25.0 $<$ WBGT $\leq$ 28.0), Caution (21.0 $<$ WBGT $\leq$ 25.0), and Safe (WBGT $\leq$ 21.0).

In this study, we specifically define "heat stress" as the WBGT levels within the categories of "Danger" and "Severe Warning", allowing us to effectively identify critical spatiotemporal heat stress exposure hotspots across India. The spatial distribution of maximum WBGT indicates that most regions across India reach the "Severe Warning" level, while some eastern areas experience conditions at the "Danger" level (Fig. 2, left).

Subsequently, we perform detailed analyses of heat stress intensity and continuity of India in year 2019 at different temporal resolutions. The maximum WBGT values in monthly level and 3-hour-interval level are calculated at the geohash level to represent areas of peak **heat exposure intensity**. Recognizing that prolonged heat stress poses severe

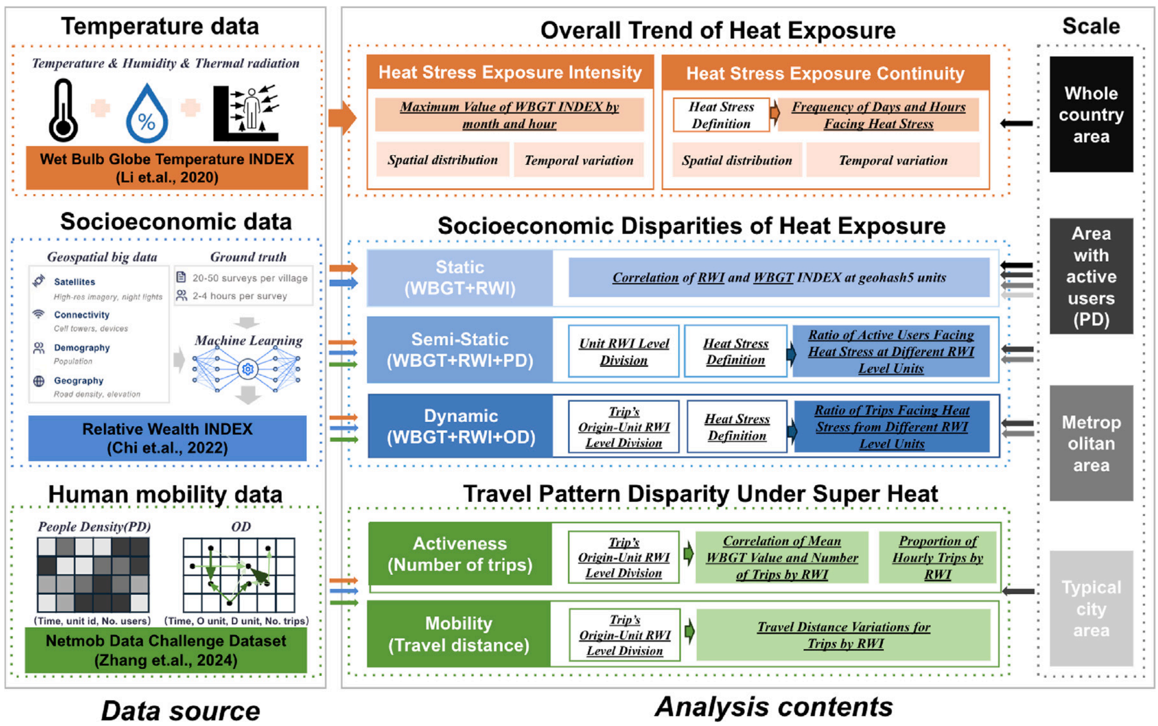

Fig. 3. Research framework.

threats to human health and urban infrastructure, we further quantify **heat exposure continuity**. Specifically, we calculate the duration during which each geohash unit continuously experiences "heat stress" risk. This measure highlights areas susceptible to persistent extreme heat conditions over extended periods.

3.3.2. Socioeconomic disparities in heat exposure

We explore socioeconomic disparities in heat exposure by integrating the Wet Bulb Globe Temperature (WBGT) index, Relative Wealth Index (RWI) data, dynamic population density, and mobility datasets. Our analysis is structured into three perspectives: static, semi-static, and dynamic.

First, we adopt a static perspective by analyzing the correlation between WBGT and RWI values at the Geohash-5 resolution across monthly and 3-hourly intervals. This analysis is conducted at four scales introduced in Section 3.1 to account for spatial heterogeneity and reduce analytical bias.

Scientific basis and scope of the exploratory intra-urban analysis. Because the city-level WBGT–RWI analysis is intended only as an exploratory assessment, it is important to clarify its scientific basis and representational limits. ERA5-Land provides spatially continuous meteorological fields at a horizontal resolution of approximately 9 km, which is not sufficient to resolve neighborhood-scale urban microclimatic variability. In particular, it cannot capture fine-scale processes such as street-canyon shading, building morphology, localized ventilation, or small-area land-cover heterogeneity. Accordingly, the intra-urban analysis presented in this study is not intended to identify neighborhood-scale heat inequity or micro-scale thermal contrasts.

At the same time, ERA5-Land-derived WBGT may still provide a limited basis for exploring broad intra-city gradients in very large urban regions. WBGT is derived from near-surface meteorological conditions, including air temperature, humidity, and radiation-related variables, and therefore reflects large-scale land–atmosphere conditions that may vary across metropolitan space. At this coarse resolution, the dataset may partially represent broad differences associated with built-up extent, vegetation scarcity, impervious surface dominance, and regional surface energy balance, as well as the contrast between denser urbanized zones and surrounding peri-urban areas. These influences are represented only in an aggregated sense and should not be interpreted as direct measures of pedestrian-scale thermal environments.

This distinction is particularly relevant in the Indian context, where several metropolitan regions are spatially extensive. In such cases, multiple ERA5-Land grid cells can span different parts of a metropolitan area and thus may capture coarse intra-metropolitan environmental gradients, even though they remain too coarse for neighborhood-scale inference. For this reason, we interpret the city-level WBGT–RWI analysis as an exploratory assessment of broad intra-city or intra-metropolitan patterns rather than a definitive analysis of intra-urban microclimatic inequality.

However, static residential-based analyses alone fail to capture the heat exposure individuals encounter through daily mobility. To address this, we incorporate dynamic population density data to assess variations in heat stress (WBGT "Danger" or "Severe Warning") exposure of users conducting activities in units of differing RWI levels during noon hours (12:00–15:00) throughout 2019. Although individual-level socioeconomic status is unavailable, we use the RWI of the location where users are active as a proxy for daytime work environment quality, assuming that higher RWI units are associated with better infrastructure and thermal protection, such as more access to cooling facilities and green spaces. This constitutes our semi-static perspective, revealing disparities in heat stress experienced across activity spaces.

Finally, we introduce an origin–destination (OD) matrix to capture the dynamic perspective of heat exposure. This allows us to compare the composition of trips made under heat stress (WBGT "Danger" or "Severe Warning") across RWI groups in the context of full daily mobility. Each trip is categorized by the RWI level of its origin unit, and WBGT values at the destination are used to determine exposure risk. This enable us to analysis how heat exposure is dynamically experienced by different socioeconomic groups during transit.

3.3.3. Travel patterns disparity under heat stress

Heat stress experienced by people across different socioeconomic groups in India may influence their mobility behavior. In particular, residents from varying wealth groups might actively or passively adjust their travel patterns in response to extreme heat. For instance, high-income individuals may have greater flexibility in their schedules or access to climate-controlled transportation and workplaces, enabling them to avoid exposure during peak heat periods. In contrast, lower-income populations might lack such flexibility, forcing them to maintain mobility even under high heat stress conditions.

To quantify these behavior adaptations and disparities, we analyze human mobility patterns through two key dimensions:

People Activeness (number of trips)

We first examine the correlation between mean WBGT levels and the number of trips conducted by different socioeconomic groups (RWI level) during midday periods (12:00–15:00), when heat exposure typically peaks. This analysis is performed at the national scale to initially understand general patterns of travel activeness under heat stress. We further explore how these behavioral responses vary temporally and spatially. Specifically, we compare differences in midday trip volumes across socioeconomic groups during hot seasons (May-August) versus cold seasons (December-February) at the geohash spatial unit scale. Additionally, we analyze variations in trip proportions across different hourly intervals throughout the day, identifying whether socioeconomic status influences adjustments in daily travel timing in response to heat exposure.

People Mobility (distance of trips)

To understand how extreme heat conditions impact travel distances, we further analyze the relationship between WBGT levels and the average trip distance across socioeconomic groups. Specifically, we assess whether elevated heat stress conditions lead to shortened travel distances as an adaptive behavior, and examine if these adaptive responses vary significantly among different wealth groups.

4. Results

4.1. Overall trend of heat exposure

4.1.1. Heat stress exposure intensity

The intensity of heat stress across India is displayed by visualizing monthly and 3-hour-interval maximum WBGT values at the geohash level (Fig. 4). The results suggest that India experiences the most severe heat stress from May to June, particularly during midday hours (12:00–15:00). Spatially, northern India experiences longer periods of heat stress from June to September, whereas southern India faces shorter heat-stress periods from April to July.

4.1.2. Heat stress exposure continuity

Fig. 5 (top) illustrates the annual frequency (total number of days) of heat stress exposure across India (a and c), along with the temporal distribution of affected areas (geohash count) under different WBGT levels (b). Eastern coastal regions experience notably longer durations of heat stress annually compared to the western regions, with certain areas such as Kolkata enduring heat stress conditions for up to 140 days per year. Temporally, the majority of heat-stress days occur between April and September, peaking in July.

Hourly variations within a day are further depicted in Fig. 5 (bottom), revealing spatial–temporal patterns of heat stress. Consistent with annual observations, hourly patterns also exhibit higher heat stress continuity in northeastern regions and lower continuity in southwestern regions. Between May and September, northeastern metropolitan area—including New Delhi, Lucknow, Patna, and Kolkata-face prolonged daily heat stress durations of over 18 h, with peak continuity observed in June. In contrast, southwestern and central regions generally experience shorter daily durations of heat stress (typically less than 6 h), predominantly concentrated around midday hours, except in major urban centers like Ahmedabad, Vadodara, Surat, and Mumbai, which show moderate heat-stress durations.

Overall, India's heat exposure is characterized by high and prolonged temperature extremes, particularly in densely populated northeastern metropolitan areas.

4.2. Socioeconomic disparities of heat exposure

4.2.1. Static perspective

Fig. 6 illustrates the correlation between the RWI and WBGT across four spatial scales, highlighting how analytical scope influences the robustness and interpretation of findings. At the national scale, both monthly and hourly maximum WBGT show weak but significant positive correlations with RWI. Given that lower RWI values typically correspond to rural areas and higher values to urbanized regions, this pattern suggests that urban areas face greater heat stress (Feng et al., 2023; Gao et al., 2024; Li et al., 2025).

However, when the analysis is restricted to the populated-area scale (areas with active users), a different trend emerges: during the hot season (May-October), RWI exhibits a weak negative correlation with maximum WBGT. This indicates that, at a broad population scale, lower-income areas may be associated with slightly higher extreme heat exposure, although the effect size is small. The magnitude of these correlations remains small, suggesting that socioeconomic factors explain only a limited portion of WBGT variability, with other environmental and urban characteristics also playing important roles.

At the metropolitan-region scale, the association between lower RWI and higher WBGT becomes somewhat stronger, with pooled correlation coefficients around $r \approx 0.3$ (Fig. 6(3)). Although statistically significant, this represents a modest relationship. Because this analysis aggregates data across diverse metropolitan regions with different climates, urban forms, and development levels, the observed correlation reflects large-scale gradients rather than uniform intra-urban patterns. These findings are therefore indicative of broad socio-environmental tendencies, consistent with previous studies reporting associations between socioeconomic disadvantage and heat exposure (Hsu et al., 2021; Li, Yigitcanlar et al., 2024), but do not imply that income alone is a dominant determinant.

Given the limited resolution of the WBGT data, we further examined the correlation between RWI and yearly maximum WBGT at the individual city scale as an exploratory assessment of coarse spatial gradients within large metropolitan areas. Results show substantial heterogeneity: most cities exhibit weak or statistically insignificant correlations, and the direction of association varies across locations, with a few southern cities (e.g., Visakhapatnam and Bengaluru) showing significant relationships. This variability suggests that socioeconomic thermal relationships are not uniform within Indian cities (Chakraborty, 2024). However, it should be noted that both the magnitude and spatial structure of these associations are influenced by data limitations. The coarse spatial representation of both RWI and WBGT restricts the detection of neighborhood-scale contrasts, and ERA5-Land-derived WBGT cannot resolve key urban microclimatic processes such as shading, building density, or street-level ventilation. As a result, these city-scale correlations should be interpreted cautiously as exploratory indicators of broad center-to-periphery gradients, rather than robust evidence of neighborhood-scale inequality.

Overall, the multi-scale analysis suggests that heat exposure patterns in India arise from the interaction of climatic, environmental, and socioeconomic processes. While modest RWI-WBGT associations are observable at aggregated population and metropolitan scales, these relationships are not consistently expressed within individual cities, highlighting the heterogeneous and multifactorial nature of urban heat exposure.

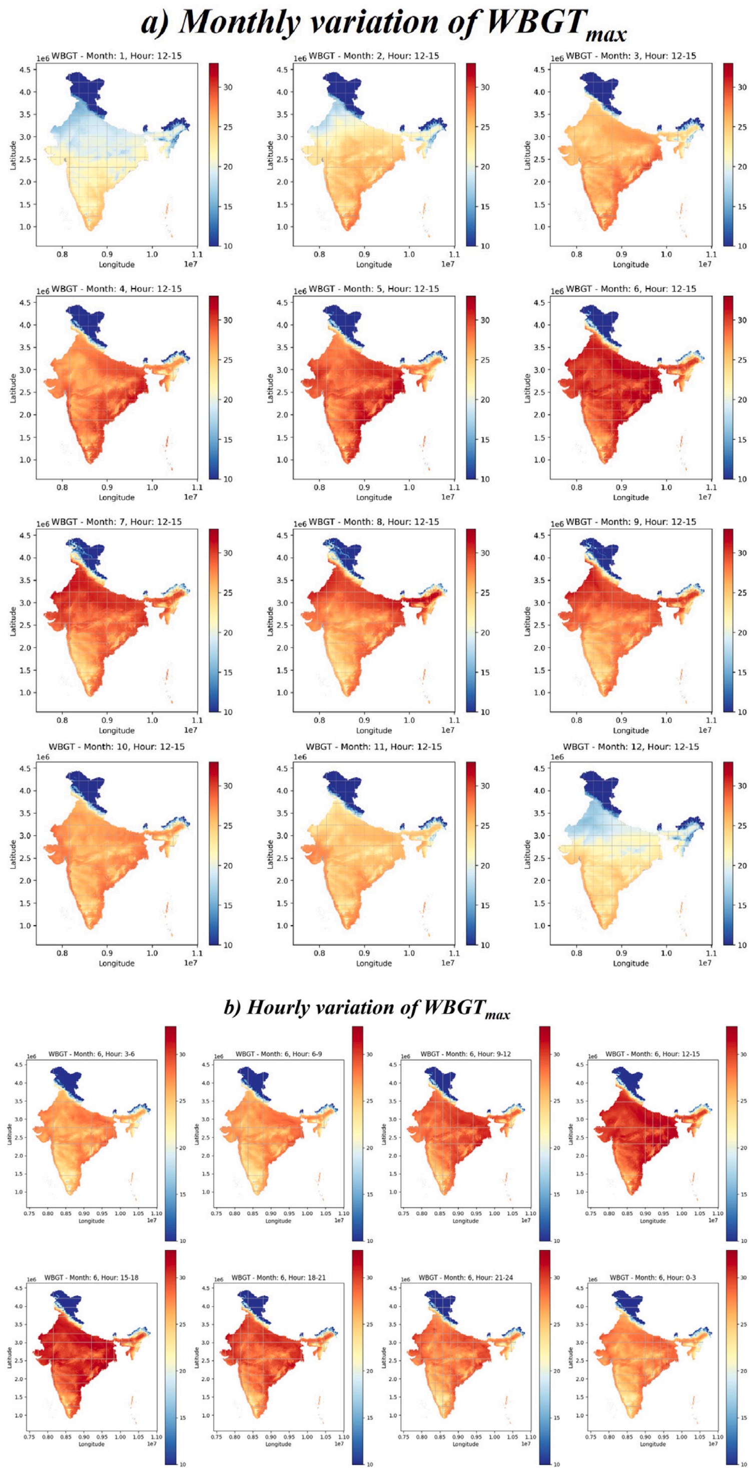

Fig. 4. Heat stress exposure intensity in India (2019).

4.2.2. Semi-static perspective

Fig. 7 and Table 1 present the proportion of users exposed to extreme heat stress (WBGT “Danger” or above) over time across different socioeconomic units and spatial scales. Exposure rates peak in June, affecting nearly 70% of users in populated areas, and over 80% within metropolitan areas-highlighting substantial population vulnerability during the hottest periods.

Independent sample t-tests confirm that users active in high-RWI units experience significantly less heat stress exposure than those in other socioeconomic units. However, exposure differences among low, mid, and mid-high RWI categories are not statistically significant. This suggests that the relationship between heat stress exposure and socioeconomic status is nonlinear: only the wealthiest environments appear to offer substantial protection. This threshold-like pattern aligns

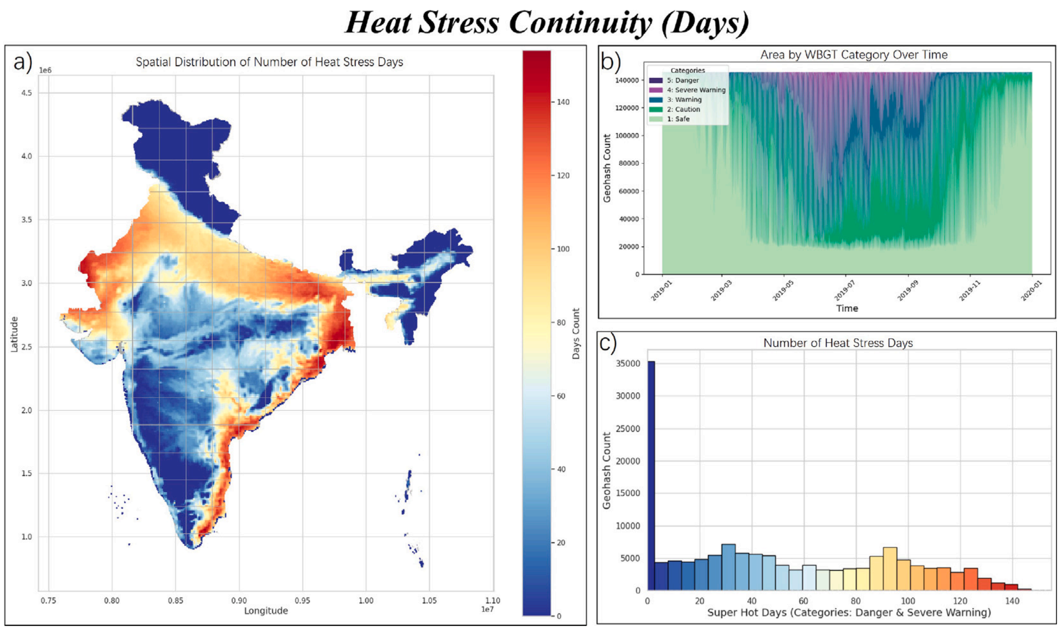

(a) (1) Monthly differences in heat stress exposure intensity.
Note: (a) Spatial distribution of number of Heat Stress days in 2019 (the day with highest WGBT index over 28); (b) Number of daily geohash units facing different heat exposure levels in 2019; (c) Number of geohashes with different length of Heat Stress days in 2019.

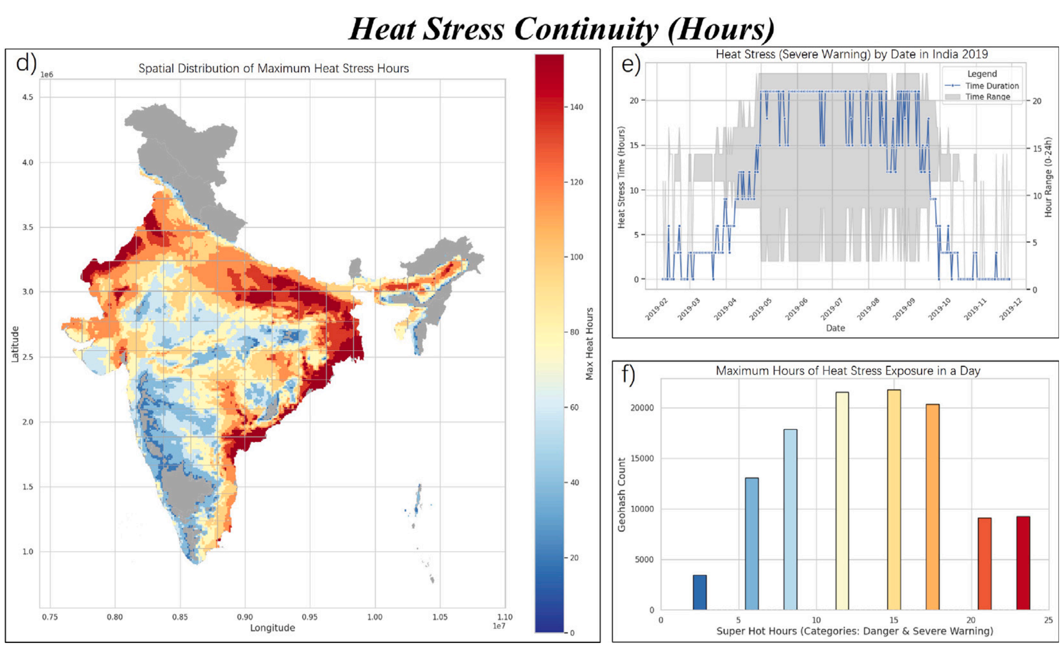

(b) (2) Three-hour-interval differences in heat stress exposure intensity.
Note: (d) Spatial distribution of longest heat stress duration during one day in 2019 (Maximum daily time duration when the highest WGBT index is over 28 in 2019); (e) Daily time and duration when heat stress happened in India in 2019 (If the WBGT index of any place in India is over 28, then we regard the India was facing heat stress); (f) Number of geohashes with different length of Heat Stress hours during one day in 2019.

Fig. 5. Heat stress exposure continuity in India (2019).

with previous studies, which indicate that the benefits of cooler microclimates are often concentrated in affluent neighborhoods (Hsu et al., 2021; Li, Yigitcanlar et al., 2024).

4.2.3. Dynamic perspective

Fig. 8 explores socioeconomic disparities in heat stress exposure (WBGT "Danger" or "Severe Warning") specifically related to trip activities. The results demonstrate that individuals from the High RWI group undertake fewer trips under extreme heat conditions during hot seasons, both at the national scale and in metropolitan areas.

However, similar to the pattern observed in the previous section, this exposure rate does not decrease proportionally with increasing RWI from the Low to Mid-High categories. In stead, the proportion of trips under heat stress appears higher in the Mid and Mid-High RWI groups

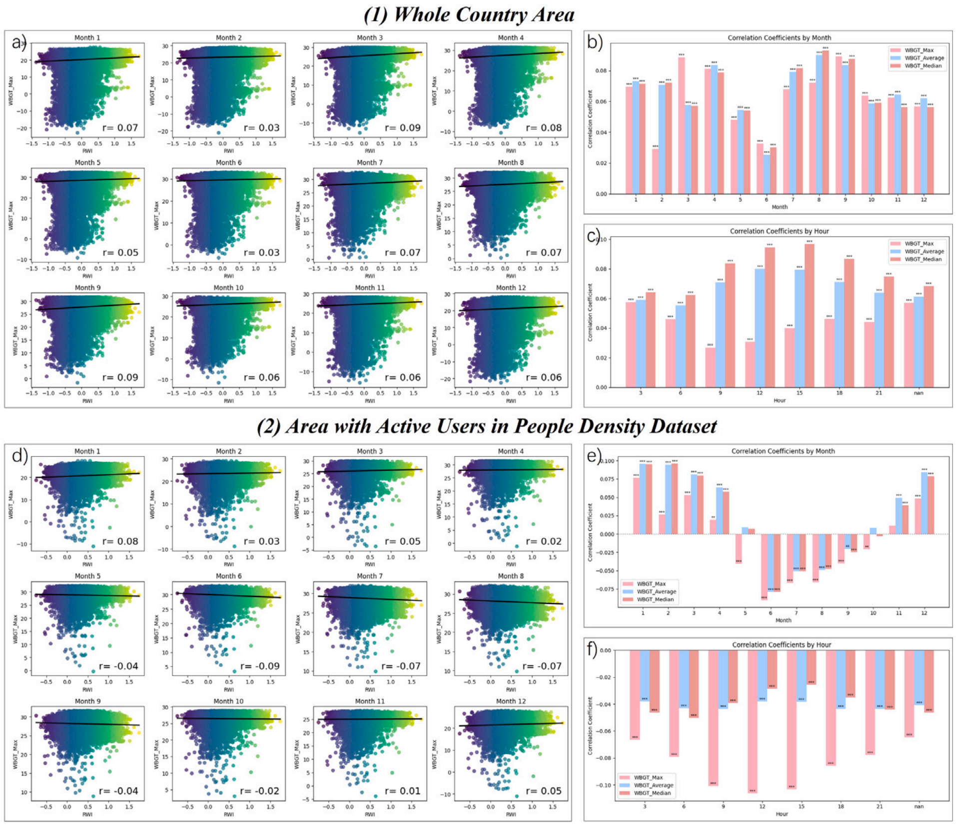

Note: (a) and (d) are Scatter plots of RWI level with Monthly WBGT in the Whole country area and Area with active users; (b) and (e) are Monthly correlation coefficients with significance levels in the Whole country area and Area with active users; (c) and (f) are Hourly correlation coefficients with significance levels in the Whole country area and Area with active users during hot seasons (Apr.-Oct.)

Fig. 6. Correlation of RWI levels with WBGT in India at Various Study Scales (2019).

Table 1
Mean ratio of users facing heat stress by month at different RWI level units.

Area	Month	Low RWI	Mid RWI	Mid-high RWI	High RWI
Area with active users	Apr.	16.31%	19.96%	15.57%	15.77%
	May.	31.61%	31.12%	25.44%	25.53%
	June.	55.78%	52.63%	59.08%	48.00%
	July.	35.63%	31.78%	39.02%	27.20%
	Aug.	28.39%	24.14%	29.68%	19.64%
	Sep.	22.74%	20.73%	26.27%	17.80%
Metropolitan area	Apr.	20.01%	15.07%	15.43%	12.26%
	May.	40.50%	28.47%	26.45%	23.42%
	June.	58.54%	54.45%	61.58%	47.20%
	July.	28.27%	31.17%	39.05%	24.33%
	Aug.	19.68%	22.78%	28.75%	16.14%
	Sep.	22.39%	24.13%	29.73%	18.01%

than in the Low RWI group. Furthermore, we observe a data gap for the Low RWI group in metropolitan areas during the hot season. This may suggest a potential reduction or limitation of trips due to severe heat stress for low RWI users.

4.3. Travel pattern disparities under heat stress

People Activeness

Fig. 9 presents the correlation between mean WBGT levels and the number of trips conducted by different socioeconomic (RWI) groups during midday hours (12:00–15:00) across India. A positive correlation between rising WBGT levels and increased trip frequency is observed consistently across all four RWI groups, aligning with the overall pattern of total daily trips (Fig. 9, right). However, this positive correlation weakens with decreasing socioeconomic levels. This indicates that lower-income groups are comparatively less likely to increase their travel activities when the temperature rise, reflecting possible mobility constraints under extreme heat conditions.

To further investigate how socioeconomic disparities in travel activeness vary seasonally and temporally, we examined the relationship between WBGT values and midday trip volumes at the geohash level during the hot (May-August) and cold (December-February) seasons for each RWI group (Fig. 10). Lower-income groups (low and mid RWI) exhibit distinct seasonal variations, showing greater sensitivity in their travel patterns to temperature changes, whereas high-income groups (mid-high and high RWI) display relatively stable travel behaviors across different seasons. This pattern suggests that economically disadvantaged populations face greater vulnerability in their travel activities during periods of extreme heat. The ability to modify one's mobility behavior in response to heat is a privilege, and neighborhoods with lower socioeconomic status are less able to enact behavioral adjustments to avoid heat exposure (Stechemesser & Wenz, 2023).

Furthermore, the proportion of trips conducted in different hourly intervals by socioeconomic groups reveals adaptive travel strategies under heat stress conditions. Fig. 11 depicts that, during hot seasons, individuals-particularly from lower-income groups-strategically shift their travel to cooler early morning (6:00–9:00) and evening (18:00–21:00) periods. This alternative time travel strategy is more pronounced in lower-income groups (RWI level). This adaptive temporal shift in mobility patterns is also prominent within metropolitan areas, underscoring the socioeconomic differentiation in coping strategies toward heat exposure.

(3) Metropolitan Area

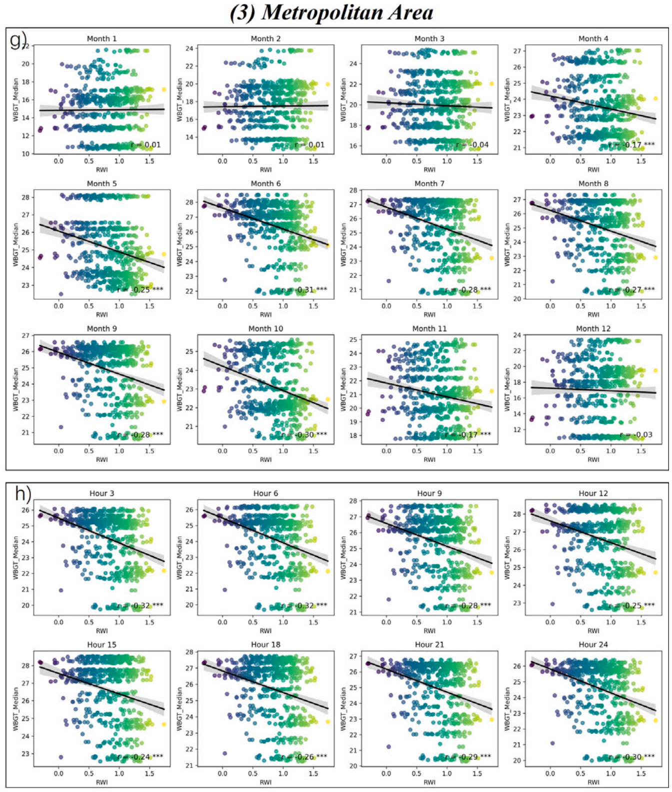

Note: (g) Scatter plots of RWI level with Monthly WBGT median in the Metropolitan area; (h) Scatter plots of RWI level with Hourly WBGT median during hot seasons (Apr.-Oct.) in the Metropolitan area.

(4) Typical Cities

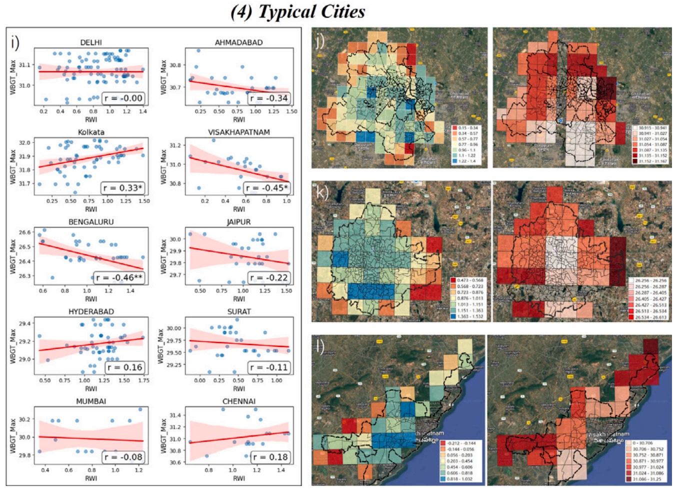

Note: (i) Scatter plots of RWI level with yearly WBGT Max value in the metropolitan area; (j), (k), (l) are the spatial distribution of RWI and WBGT index in Delhi, Bengaluru and Visakhapatnam city respectively; ***99.9% confidence, *95% confidence.

Fig. 6. (*continued*).

This differentiated activeness highlights a paradox in heat exposure behaviors. On the one hand, residents from lower-income areas experience higher daily heat exposure, encouraging them to reduce activities during peak heat periods. On the other hand, higher-income groups, benefiting from greater accessibility to urban amenities, cooler public spaces, and air-conditioned transportation, maintain more consistent activity patterns that are less impacted by extreme heat.

People Mobility

Fig. 12 and Table 2 illustrate various in travel distances across different socioeconomic groups. The analysis reveals distinct differences among RWI groups in their mobility patterns as the standard deviation is relatively high across all groups. The Low RWI group generally undertakes shorter average trip distances, reflecting daily necessities such as shopping or daily commuting occurring within proximate areas. However, the high standard deviation (14,717 m) within this group suggests considerable variability, indicating that certain low-income residents must travel long distances, likely to access essential services like employment opportunities or healthcare facilities.

In contrast, high and mid-high RWI groups exhibit consistently longer average trip distance, with a relatively lower standard deviation (11,799 m). This indicates that residents from wealthier regions tend to have more consistent mobility patterns, potentially benefiting from better access to urban infrastructures in closer proximity to their locations.

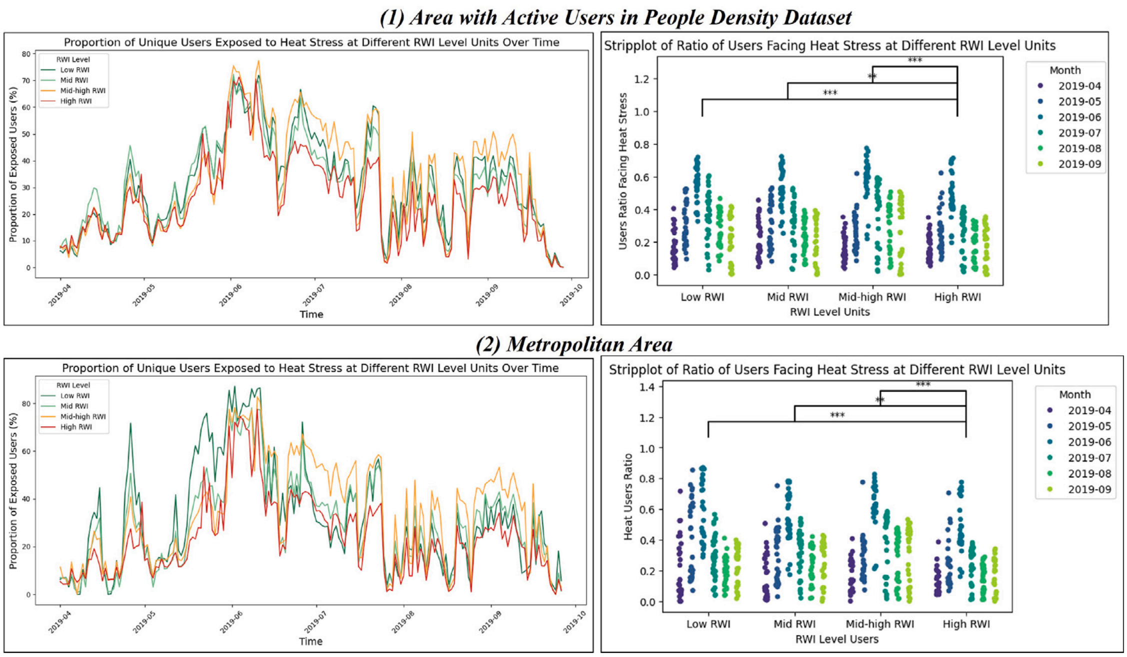

Fig. 7. Proportion of users facing heat stress at different RWI level units over time.

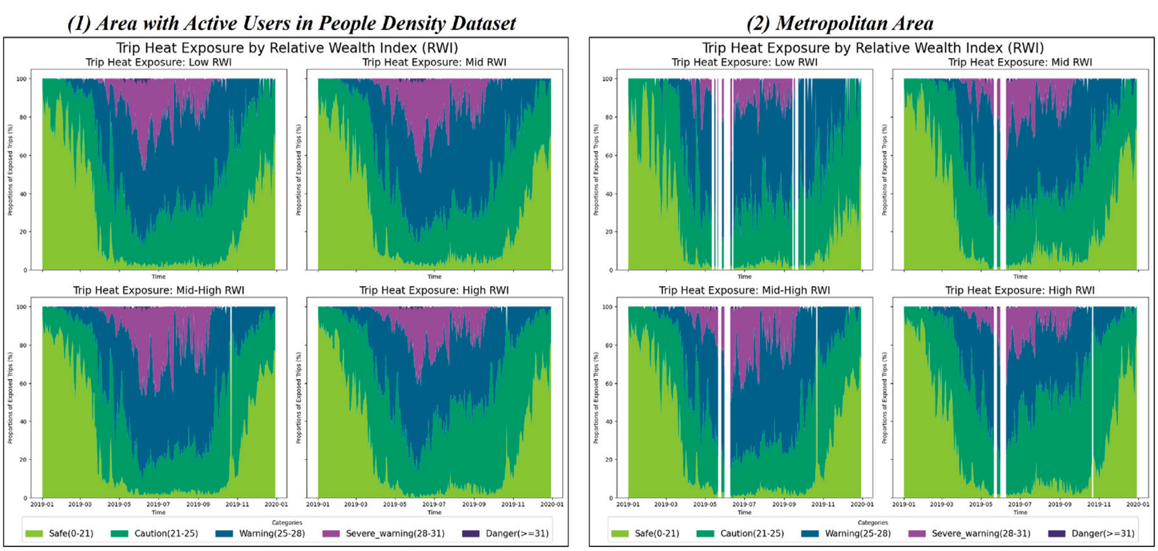

Fig. 8. Proportion of trips facing heat stress by RWI level over time (2019).

Overall, travel distances tend to be slightly longer during hot seasons compared to cold seasons. However, no clear relationship was identified between WBGT level and relative changes in travel distance among socioeconomic groups. The relative differences in average trip distances across four RWI groups remained stable irrespective of seasonal variations or hourly periods (Fig. 12). These findings suggest that travel distance is largely decided by underlying mobility capabilities and socioeconomic constraints, and remains relatively unaffected by changes in heat stress conditions.

Table 2
Trip distance descriptive statistics by RWI levels.

Statistic	Low RWI	Mid RWI	Mid-high RWI	High RWI
Count	99,377	332,550	456,979	475,543
Mean	3834	3833	3982	3914
Std.	14,717	12,378	11,956	11,799
Min	84	96	86	123
25%	971	1249	1483	1564
Median	1642	2006	2303	2423
75%	3124	3516	3852	3996
Max	1.43×10^6	1.17×10^6	1.33×10^6	1.41×10^6

5. Discussion

This study proposes a systematic, multi-scale analysis of heat exposure patterns across India in 2019, integrating high-resolution, dynamic human mobility data. The findings provide new insights on how socioeconomic disparities shape heat exposure in developing countries, addressing a major research gap in climate-health and urban equity studies.

Our analysis identifies clear spatial and temporal trends in extreme heat across India, underscoring urgent public health challenges. The hourly and monthly resolution enhance the understanding of short-term

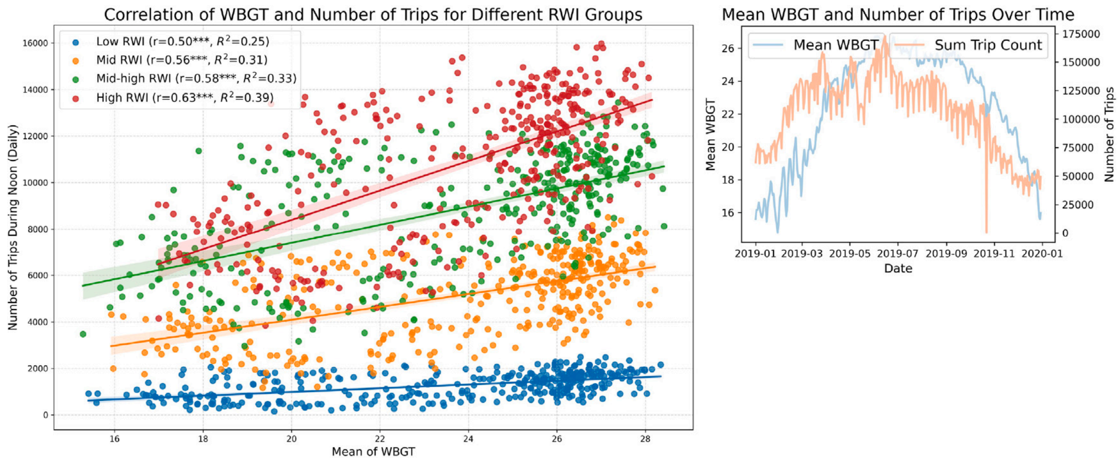

Fig. 9. Correlation of daily mean WBGT value and daily number of trips (midday time) by RWI groups in the area with active users.

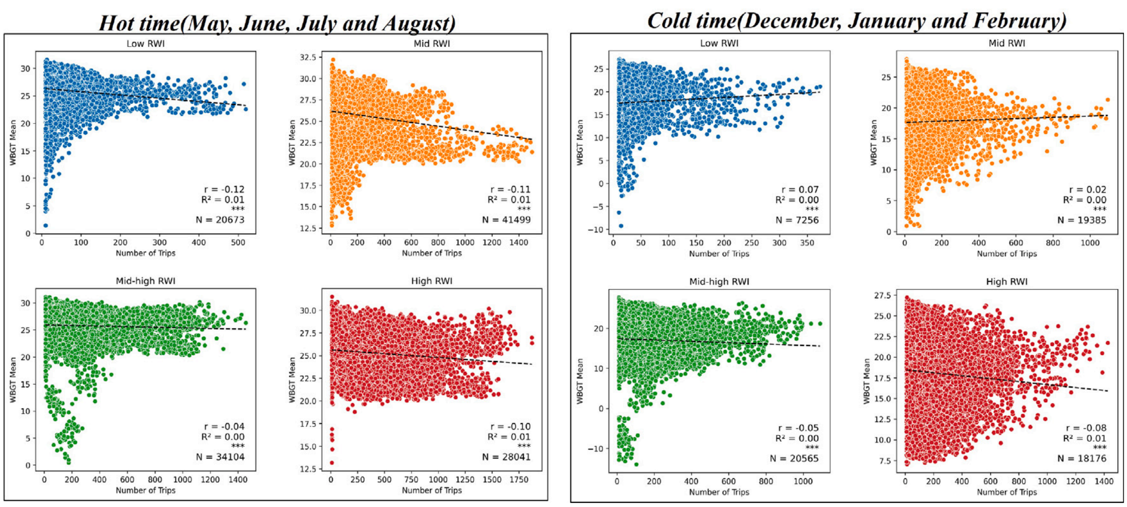

Fig. 10. Correlation of daily mean WBGT value and daily number of trips (midday time) by RWI groups during hot and cold time at geohash scale.

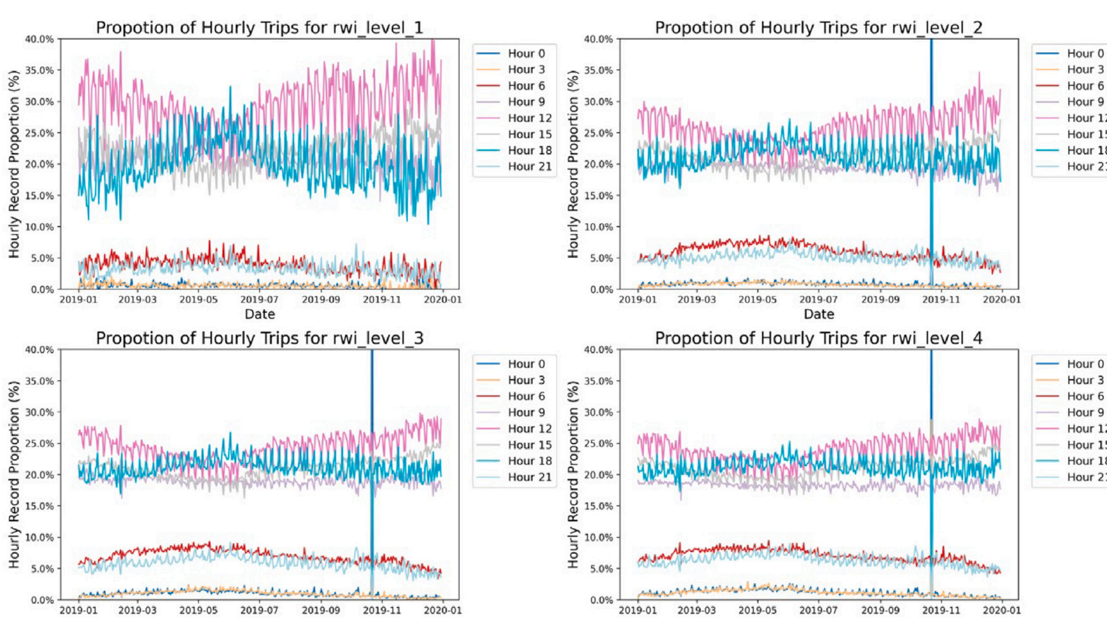

Fig. 11. Proportion of hourly trips by RWI groups over time.

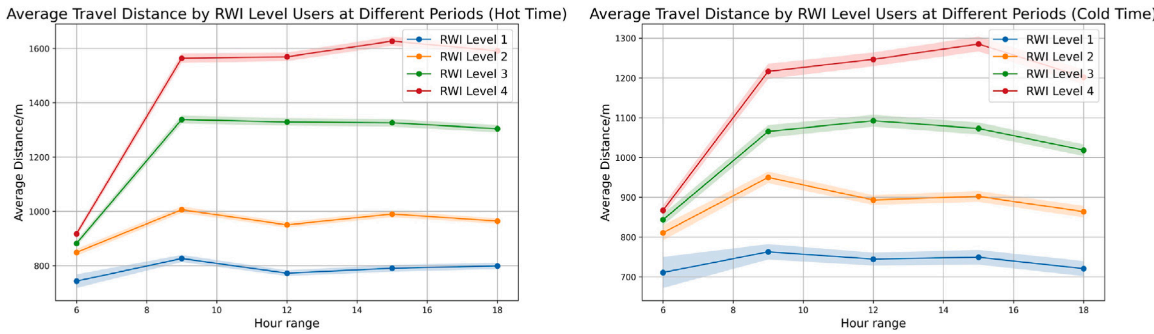

Fig. 12. Average travel distance of trips by RWI groups during hot and cold time with 95% confidence interval.

fluctuations in heat exposure, allowing for more timely and spatially precise policy interventions. This insights can support urban policymakers and planners in designing proactive measures such as early warning systems, medical preparedness, public awareness campaigns, cooling centers, or adjustments to public service schedules during peak heat hours (Hess et al., 2023).

A key contribution of this study lies in examining socioeconomic indicators relate to heat exposure across multiple spatial and analytical scales. At the aggregated population and metropolitan scales, lower-income areas tend to be associated with slightly higher levels of heat exposure, particularly within large urban regions. Although the correlation coefficients are modest, their magnitude is comparable to those reported in other socio-environmental exposure studies (Li, Wang et al., 2024; Raj et al., 2025; Yin et al., 2023). Moreover, our analysis spans metropolitan areas across diverse climatic zones, urban forms, and development histories in India. Such heterogeneity may also reduce pooled correlation strength compared with single-city case studies with smaller samples.

Additionally, the magnitude and direction of RWI–WBGT relationships vary across 21 metropolitan cities. While some cities display negative associations and others positive, most city-level correlations are weak or statistically insignificant. This inter-city variability is consistent with emerging evidence from Global South cities suggesting that socioeconomic gradients in heat hazard are highly context-dependent and may differ from commonly observed U.S. patterns (Chakraborty, 2024). Similar heterogeneity has also been reported in comparative analyses across cities such as Seoul and London (Raj et al., 2025), indicating that relationships between socioeconomic level and heat exposure depend on local development pathways, urban structure, and environmental conditions (Raj et al., 2025; Yin et al., 2023).

However, given the coarse spatial resolution of both WBGT and RWI, these results should be interpreted with caution. ERA5-Land does not resolve urban microclimatic variability, and RWI has not been validated as a neighborhood-scale socioeconomic indicator within cities. Accordingly, these individual city analyses are intended as exploratory and hypothesis-generating, should not be interpreted as evidence of neighborhood-scale heat inequality. Future research using higher-resolution urban climate data, detailed building-scale information, and validated intra-urban socioeconomic data will be essential to more precisely assess heat exposure disparities within cities.

In India, several factors make urban populations particularly vulnerable to extreme heat: the prevalence of informal housing without thermal insulation, limited public access to cooling infrastructure, irregular electricity supply, and a large informal workforce engaged in outdoor labor without schedule flexibility. Additionally, many low-income neighborhoods lack sufficient green cover, water infrastructure, or healthcare services, exacerbating the health risks posed by rising temperatures. These challenges are compounded by rapid urbanization and governance fragmentation, which often hinder the equitable implementation of heat mitigation measures. Therefore, to address these inequalities in India's context, community-based strategies should be utilized, and the most vulnerable groups should be prioritized, including slum dwellers, daily wage workers, and elderly populations in high-density low-resource settings. Potential strategies include the increase of green infrastructure (e.g., improvements in housing quality and thermal insulation, enhanced public cooling facilities (Xiong & He, 2024), and parks, green roofs, and urban forests) (Probst et al., 2022).

Extending from the semi-static to the dynamic perspective, the integration of human mobility data reveals that lower-income groups face higher exposure during travel, while displaying more pronounced changes in mobility patterns during heat events. At first glance, these variations might appear adaptive—for instance, shifting travel to early-morning or evening hours. However, our study does not capture trip purpose or behavioral intent, and thus we refrain from categorizing these responses as definitive "adaptive strategies". Instead, we interpret them as potential indicators of constrained behavioral flexibility, shaped by limited access to cooling infrastructure, inflexible work hours, or reduced transportation choices. This aligns with Stechemesser and Wenz (2023), who argue that behavioral flexibility is itself a form of privilege, and that neighborhoods with lower socioeconomic status are often less able to enact mobility-based adjustments under heat stress.

While studies such as Tang et al. (2023) show that during short-term extreme events like floods, mobility changes among different demographic groups can clearly function as coping or adaptive mechanisms, heat exposure can instead be understood as chronic in terms of cumulative exposure and structural vulnerability, even though individual heatwave events themselves are acute. From this perspective, mobility variability under heat may reflect longer-term structural constraints rather than short-term adaptive responses.

Additionally, observed differences in trip distances across socioeconomic groups are likely driven by broader structural inequalities in urban infrastructure, mobility resources, and service accessibility, which indirectly influence individuals' ability to avoid or mitigate exposure to heat.

Interestingly, this creates an apparent paradox: despite urban centers typically exhibiting higher surface temperatures due to the urban heat island effect, wealthier urban residents may experience lower actual heat stress due to their greater financial capacity to mitigate heat (e.g., through air conditioning and private transportation) (Wu et al., 2024). Conversely, residents in low-income urban settlements or slum areas adjacent to urban cores face compounded vulnerabilities, confronting both the urban heat island effect and limited adaptive capacities. Future research should specifically target these vulnerable communities to accurately capture their lived heat exposure experiences and develop targeted intervention measures.

While this study provides comprehensive analyses leveraging mobility and environmental data, several limitations should be noted.

Firstly, the mobility data utilized in this study is derived from mobile application logs and aggregated at the Geohash-5 level (Zhang et al., 2024). Smartphone-based data may systematically underrepresent certain demographic groups, such as elderly populations or very low-income individuals without access to smartphones (Tang et al., 2023). Unfortunately, these underrepresented groups constitute a significant and critical segment of the population in many developing countries, and their exclusion may overlook critical vulnerabilities. Future research should urgently address this challenge. Additionally, population density (PD) data used in this study was not directly calibrated against official census data, which may also lead to bias in the analysis. Moreover, the mobility dataset including PD and OD data are aggregated at a relative large unit (geohash 5 unit) which limits its application in a smaller scale analysis such as inner-city heat exposure study. Future research could integrate multiple complementary data sources, such as census-based demographic information and household surveys, to validate and enhance the representativeness of mobile-based mobility data. Additionally, methods such as spatial disaggregation or microsimulation modeling could improve data coverage, especially among underrepresented rural and low-income populations.

Second, while this study explores temporal and spatial patterns of mobility under extreme heat, we acknowledge that the absence of trip purpose data limits our ability to directly attribute such patterns to coping or adaptation behaviors. Human mobility is influenced by a variety of factors, such as work obligations, access to services, and cultural or familial responsibilities, that may or may not be directly responsive to temperature changes. Therefore, our findings should be interpreted as possible behavioral constraints or responses to heat stress, rather than definitive coping strategies. Future research that incorporates trip purpose or occupational data will be essential to more precisely characterize adaptive behaviors under extreme heat.

Third, our study relies on the RWI as a proxy for local socioeconomic status, it carries inherent uncertainty. It is derived from machine learning models based on non-traditional data sources such as satellite imagery. These models may exhibit regional performance variation and do not capture intra-neighborhood inequality. Accordingly, RWI is used in this study as a coarse indicator of relative socioeconomic position rather than a direct measure of income or wealth. To account for these limitations, we adopted a quartile-based classification to mitigate this uncertainty and performed multi-scale and multi-perspective analyses to enhance robustness, and we interpret individual city analysis results as exploratory rather than confirmatory. Supplementary analyses comparing RWI with DHS household wealth data further illustrate the challenges of validating socioeconomic proxies at intra-urban scales in India and support the exploratory interpretation adopted in this study (Appendix).

Fourth, our environmental data source, ERA5-land, has limited spatial resolution and cannot fully capture intra-urban microclimatic variation and policy relevance. In addition, some geohash units classified as part of metropolitan areas may include mixed urban, peri-urban land cover. We explicitly acknowledged this constraint and emphasized our study's macro-level focus. Nonetheless, future studies using higher-resolution urban climate products, detailed land cover data, and refined urban boundary definitions will be essential to more precisely evaluate intra-urban socioeconomic disparities in heat exposure.

Despite these limitations, we believe this study provides a scalable methodological framework for exploring heat exposure patterns using accessible mobility data and open datasets, especially within developing country contexts where high-quality big data remains limited, thus representing a valuable contribution to urban planning and climate adaptation research globally.

6. Conclusion

This study develops a novel multi-scale and multi-perspective framework for assessing socioeconomic disparities in heat exposure by integrating temperature, human mobility, and socioeconomic data. Using India as the case study, we combined multi-source datasets at a fine spatiotemporal resolution (geohash-5 level and 3-hour intervals for 2019).

Our findings reveal clear spatiotemporal patterns of heat exposure and suggest that socioeconomic conditions are associated with differences in exposure, particularly across densely populated metropolitan regions. By quantifying disparities from static, semi-static, and dynamic perspectives, we examined how heat stress influences human mobility patterns among different socioeconomic groups. The key conclusions are as follows:

(1) Lower-income communities tend to experience slightly higher and more persistent heat stress at aggregated population and metropolitan scales, although the strength of these associations is modest and varies across cities.
(2) In addition to higher static exposure, lower-income groups also encounter greater heat stress during daily trips, suggesting constrained behavioral flexibility in avoiding heat due to infrastructural or economic limitations.
(3) Temporal shifts in trip patterns (e.g., toward cooler hours) were observed among low-income populations; however, without trip purpose data, such behaviors cannot be definitively interpreted as adaptive strategies.
(4) Differences in trip distances reflect underlying structural inequalities, with lower-income groups tend to make shorter, more variable trips, while higher-income groups maintain longer and more stable travel patterns.
(5) Despite limitations in proxy indicators such as the Relative Wealth Index (RWI), the proposed framework offers a transferable approach for assessing climate vulnerability and mobility equity in developing regions with limited data accessibility. This methodology can inform future diagnostic efforts and support inclusive urban planning.

CRediT authorship contribution statement

Jue Ma: Writing – review & editing, Writing – original draft, Validation, Methodology, Formal analysis, Data curation, Conceptualization. **Chenchen Sun:** Writing – review & editing, Visualization, Methodology, Conceptualization. **Santiago Garcia Gabilondo:** Validation, Formal analysis, Data curation. **Carl Torbjörnsson:** Formal analysis, Data curation. **Qiang Guo:** Conceptualization. **Yuya Shibuya:** Supervision, Project administration. **Yoshihide Sekimoto:** Supervision, Resources, Project administration.

Declaration of competing interest

The authors declare that they have no known competing financial interests or personal relationships that could have appeared to influence the work reported in this paper.

Acknowledgments

The authors would like to express their sincere gratitude to Cuebiq, the World Bank, and the organizers of NetMob 2024 for facilitating access to the data used in this research.

Appendix. Validation of the relative wealth index using DHS household data

To address concerns regarding whether the Relative Wealth Index (RWI) captures income or wealth distributions at intra-urban scales in India, we conducted supplementary analyses using household-level socioeconomic data from the National Family Health Survey (NFHS-5, 2019–2021), provided through the Demographic and Health Surveys (DHS) Program. These analyses assess the extent to which gridded RWI values correspond to independently collected household wealth indicators within selected large metropolitan areas.

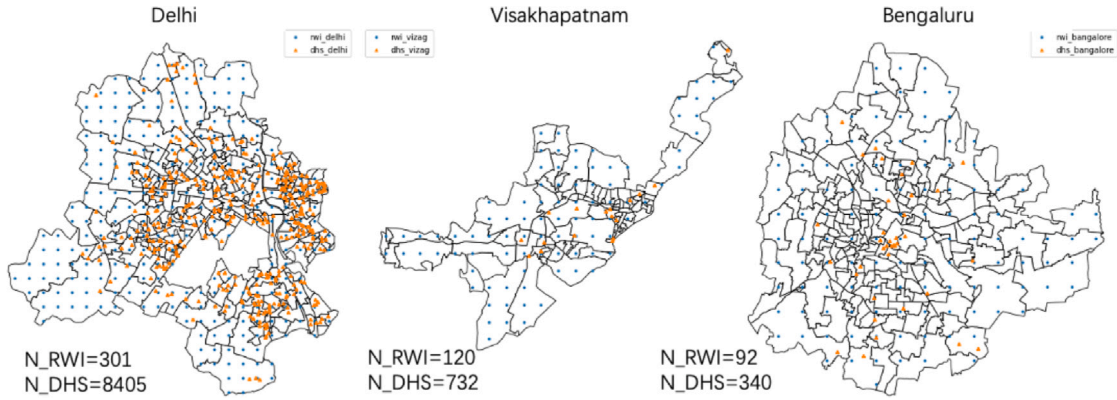

Fig. 13. Spatial distribution of DHS household samples and RWI grids within selected metropolitan areas.

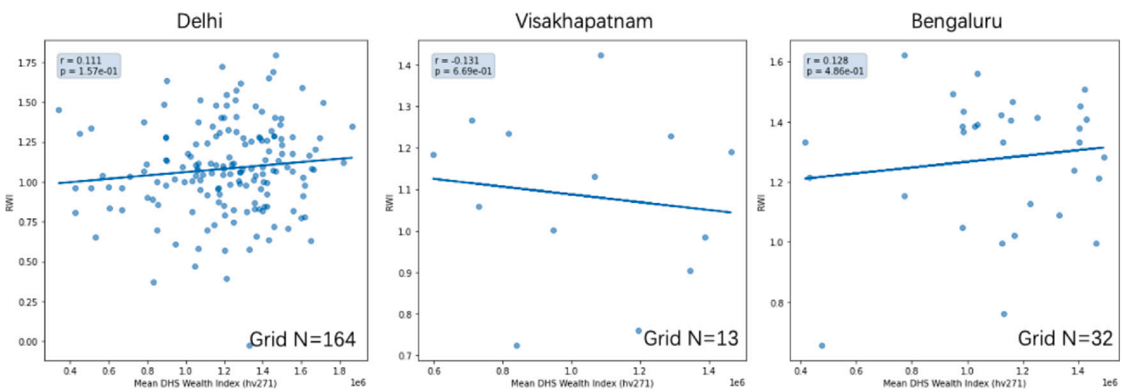

Fig. 14. Intra-urban correlations between DHS household wealth index and RWI within Delhi, Bengaluru, and Visakhapatnam.

The DHS provides nationally representative household survey data, including a standardized wealth index constructed from asset ownership, housing characteristics, and access to basic services. Unlike RWI, which offers near-complete spatial coverage at a gridded resolution across India, DHS data consist of sampled household clusters represented as point locations, with spatial displacement applied for privacy protection.

We focus on three large metropolitan cities with relatively dense DHS urban samples: Delhi (N = 8405 households), Bengaluru (N = 340 households), and Visakhapatnam (N = 732 households). To enable spatial comparison with RWI, DHS household observations were aggregated to a 250 m grid, and correlations were computed between mean DHS wealth index values and corresponding RWI values at the grid level. At the national scale, correlations were calculated using all available urban DHS samples. At the city scale, correlations were examined separately within each metropolitan area.

To illustrate spatial coverage, DHS household points and RWI grids were jointly visualized within administrative city boundaries. As shown in Fig. 13, DHS sampling is spatially uneven and does not cover all grid cells within cities; consequently, city-level analyses rely on a limited number of grid cells containing DHS observations.

At the national scale, DHS wealth index values and RWI exhibit a moderate positive correlation ($r \approx 0.59$), indicating that RWI captures broad socioeconomic gradients across India. This finding is consistent with the intended design of RWI as a large-scale proxy for relative socioeconomic position. However, at the intra-urban scale, correlations between DHS wealth and RWI are weak and statistically unstable across the three cities examined (Fig. 14). City-level correlation coefficients range from small positive to small negative values, with no consistent direction or statistical significance. This variability reflects both the limited and uneven spatial coverage of DHS sampling within cities and the coarse resolution of gridded RWI relative to neighborhood-scale socioeconomic heterogeneity.

During the preparation of this manuscript, the author(s) used ChatGPT to assist with language editing and text refinement. After using this tool, the author(s) carefully reviewed and edited the content as necessary and take full responsibility for the final content of the published article.

Data availability

The datasets used in this study are publicly available or accessible upon request:

1. Human mobility data were provided by Cuebiq and the World Bank as part of the NetMob 2024 Data Challenge. Access requires registration and approval for academic use.

2. Temperature data were obtained from the ERA5-Land reanalysis dataset provided by the Copernicus Climate Data Store, available at: https://cds.climate.copernicus.eu/datasets/reanalysis-era5-land

3. Relative Wealth Index (RWI) data were provided by Meta's Data for Good program and are available at: https://dataforgood.facebook.com/dfg/tools/relative-wealth-index

4. Household-level socioeconomic data used for supplementary analyses were obtained from the National Family Health Survey (NFHS-5, 2019–2021) through the Demographic and Health Surveys (DHS) Program. These data are available free of charge for academic research upon registration and approval by the DHS Program and are subject to the DHS Terms of Use. The data cannot be publicly redistributed

and must be accessed directly from the DHS Program website (https://dhsprogram.com).

All data were used in accordance with the terms and conditions of the respective data providers.

References

Aubrecht, C., & Özceylan, D. (2013). Identification of heat risk patterns in the us national capital region by integrating heat stress and related vulnerability. *Environment International*, *56*, 65–77.

Basu, R., & Samet, J. M. (2002). An exposure assessment study of ambient heat exposure in an elderly population in Baltimore, Maryland. *Environmental Health Perspectives*, *110*, 1219–1224.

Campbell-Lendrum, D., & Corvalán, C. (2007). Climate change and developing-country cities: implications for environmental health and equity. *Journal of Urban Health*, *84*, 109–117.

Chakraborty, T. (2024). Higher urban heat hazard in wealthierneighborhoods in the global south. http://dx.doi.org/10.21203/rs.3.rs-4461139/v1.

Chapman, D., Nilsson, K., Larsson, A., & Rizzo, A. (2017). Climatic barriers to soft-mobility in winter: Luleå, sweden as case study. *Sustainable Cities and Society*, *35*, 574–580. http://dx.doi.org/10.1016/j.scs.2017.09.003, URL: https://www.sciencedirect.com/science/article/pii/S2210670716305583.

Chen, K., Boomsma, J., & Holmes, H. A. (2023). A multiscale analysis of heatwaves and urban heat islands in the western us during the summer of 2021. *Scientific Reports*, *13*, 9570.

Chi, G., Fang, H., Chatterjee, S., & Blumenstock, J. E. (2022). Microestimates of wealth for all low-and middle-income countries. *Proceedings of the National Academy of Sciences*, *119*, Article e2113658119.

Copernicus Climate Change Service (2025). ERA5-land hourly data from 1950 to present. http://dx.doi.org/10.24381/cds.e2161bac, URL: https://cds.climate.copernicus.eu/datasets/reanalysis-era5-land?tab=overview. (Accessed 17 October 2025).

El Kenawy, A. M., Aboelkhair, H., Mohamed, E. K., Gaber, I. M., Fernández-Duque, B., Peña-Angulo, D., & Abdelaal, M. M. (2024). Modes of summertime thermal urban stress over major cities in the middle east: A comprehensive assessment of heat exposure risks. *Sustainable Cities and Society*, *102*, Article 105236.

Feng, R., Wang, F., Liu, S., Qi, W., Zhao, Y., & Wang, Y. (2023). How urban ecological land affects resident heat exposure: Evidence from the mega-urban agglomeration in China. *Landscape and Urban Planning*, *231*, Article 104643.

Gao, S., Chen, Y., Chen, D., He, B., Gong, A., Hou, P., Li, K., & Cui, Y. (2024). Urbanization-induced warming amplifies population exposure to compound heatwaves but narrows exposure inequality between global north and south cities. *NPJ Climate and Atmospheric Science*, *7*, 154.

Gu, X., Chen, P., & Fan, C. (2024). Socio-demographic inequalities in the impacts of extreme temperatures on population mobility11this research received no specific grant from any funding agency, commercial or not-for-profit sectors. *Journal of Transport Geography*, *114*, Article 103755. http://dx.doi.org/10.1016/j.jtrangeo.2023.103755, URL: https://www.sciencedirect.com/science/article/pii/S0966692323002272.

Gubernot, D. M., Anderson, G. B., & Hunting, K. L. (2014). The epidemiology of occupational heat exposure in the United States: a review of the literature and assessment of research needs in a changing climate. *International Journal of Biometeorology*, *58*, 1779–1788.

Guo, Q., Mistry, M. N., Zhou, X., Zhao, G., Kino, K., Wen, B., Yoshimura, K., Satoh, Y., Cvijanovic, I., Kim, Y., Ng, C. F. S., Vicedo-Cabrera, A. M., Armstrong, B., Urban, A., Katsouyanni, K., Masselot, P., Tong, S., Sera, F., Huber, V., ... Multi-Country Multi-City (MCC) Collaborative Research Network (2024). Regional variation in the role of humidity on city-level heat-related mortality. *PNAS Nexus*, *3*, Article gae290. http://dx.doi.org/10.1093/pnasnexus/pgae290, arXiv:https://academic.oup.com/pnasnexus/article-pdf/3/8/pgae290/58831283/pgae290.pdf.

Guo, Q., Yuan, L., Ng, C. F. S., & Hashizume, M. (2024). Evaluating Japan's revised heat-health warning system in the face of recent escalating heat stress. *Environmental Research Letters*, *19*, Article 054002.

Hatchett, B. J., Benmarhnia, T., Guirguis, K., VanderMolen, K., Gershunov, A., Kerwin, H., Khlystov, A., Lambrecht, K. M., & Samburova, V. (2021). Mobility data to aid assessment of human responses to extreme environmental conditions. *The Lancet Planetary Health*, *5*, e665–e667. http://dx.doi.org/10.1016/S2542-5196(21)00261-8, URL: https://www.sciencedirect.com/science/article/pii/S2542519621002618.

Hess, J. J., Errett, N. A., McGregor, G., Busch Isaksen, T., Wettstein, Z. S., Wheat, S. K., & Ebi, K. L. (2023). Public health preparedness for extreme heat events. *Annual Review of Public Health*, *44*, 301–321. http://dx.doi.org/10.1146/annurev-publhealth-071421-025508, URL: https://www.annualreviews.org/content/journals/10.1146/annurev-publhealth-071421-025508.

Hondula, D. M., Balling, R. C., Andrade, R., Scott Krayenhoff, E., Middel, A., Urban, A., Georgescu, M., & Sailor, D. J. (2017). Biometeorology for cities. *International Journal of Biometeorology*, *61*, 59–69.

Hsu, A., Sheriff, G., Chakraborty, T., & Manya, D. (2021). Disproportionate exposure to urban heat island intensity across major us cities. *Nature Communications*, *12*, 2721.

Jacobs, C., Singh, T., Gorti, G., Iftikhar, U., Saeed, S., Syed, A., Abbas, F., Ahmad, B., Bhadwal, S., & Siderius, C. (2019). Patterns of outdoor exposure to heat in three south Asian cities. *Science of the Total Environment*, *674*, 264–278. http://dx.doi.org/10.1016/j.scitotenv.2019.04.087, URL: https://www.sciencedirect.com/science/article/pii/S0048969719316079.

Jay, O., & Kenny, G. P. (2010). Heat exposure in the Canadian workplace. *American Journal of Industrial Medicine*, *53*, 842–853.

Karsai, M., Kertész, J., & Espín-Noboa, L. (2024). A comparative analysis of wealth index predictions in Africa between three multi-source inference models. arXiv preprint arXiv:2408.01631.

Kikumoto, H., Ooka, R., & Arima, Y. (2016). A study of urban thermal environment in Tokyo in summer of the 2030s under influence of global warming. *Energy and Buildings*, *114*, 54–61.

Kim, Y. H., Min, S. K., Zhang, X., Zwiers, F., Alexander, L. V., Donat, M. G., & Tung, Y. S. (2016). Attribution of extreme temperature changes during 1951–2010. *Climate Dynamics*, *46*, 1769–1782.

Kitchley, J. L., et al. (2024). A framework to assess the contextual composite heat vulnerability index for a heritage city in India-a case study of Madurai. *Sustainable Cities and Society*, *101*, Article 105119.

Kjellstrom, T., Holmer, I., & Lemke, B. (2009). Workplace heat stress, health and productivity–an increasing challenge for low and middle-income countries during climate change. *Global Health Action*, *2*, 2047.

Klingelhöfer, D., Braun, M., Brüggmann, D., & Groneberg, D. A. (2023). Heatwaves: does global research reflect the growing threat in the light of climate change? *Globalization and Health*, *19*, 56. http://dx.doi.org/10.1186/s12992-023-00955-4.

Kovats, R. S., & Hajat, S. (2008). Heat stress and public health: a critical review. *Annual Review of Public Health*, *29*, 41–55.

Kyaw, A. K., Hamed, M. M., Kamruzzaman, M., & Shahid, S. (2023). Spatiotemporal changes in population exposure to heat stress in South Asia. *Sustainable Cities and Society*, *93*, Article 104544. http://dx.doi.org/10.1016/j.scs.2023.104544, URL: https://www.sciencedirect.com/science/article/pii/S2210670723001555.

Laue, F., Adegun, O. B., & Ley, A. (2022). Heat stress adaptation within informal, low-income urban settlements in Africa. *Sustainability*, *14*, http://dx.doi.org/10.3390/su14138182, URL: https://www.mdpi.com/2071-1050/14/13/8182.

Lemke, B., & Kjellstrom, T. (2012). Calculating workplace wbgt from meteorological data: a tool for climate change assessment. *Industrial Health*, *50*, 267–278. http://dx.doi.org/10.2486/indhealth.ms1352, epub 2012 May 30.

Li, T., Song, F., De Cock, A., De Maeyer, P., Bao, J., Yuan, Y., Naibi, S., Bao, A., Ho, L. T., & Goethals, P. (2025). Global disparities in rural and urban population exposure to compound drought and heatwave events. *NPJ Climate and Atmospheric Science*, *8*, 207.

Li, Y., Svenning, J. C., Zhou, W., Zhu, K., Abrams, J. F., Lenton, T. M., Ripple, W. J., Yu, Z., Teng, S. N., Dunn, R. R., et al. (2024). Green spaces provide substantial but unequal urban cooling globally. *Nature Communications*, *15*, 7108.

Li, X., Wang, G., Zaitchik, B., Hsu, A., & Chakraborty, T. (2024). Sensitivity and vulnerability to summer heat extremes in major cities of the United States. *Environmental Research Letters*, *19*, Article 094039. http://dx.doi.org/10.1088/1748-9326/ad6c64.

Li, F., Yigitcanlar, T., Nepal, M., Nguyen, K., Dur, F., & Li, W. (2024). Assessing heat vulnerability and multidimensional inequity: Lessons from indexing the performance of Australian capital cities. *Sustainable Cities and Society*, *115*, Article 105875. http://dx.doi.org/10.1016/j.scs.2024.105875, URL: https://www.sciencedirect.com/science/article/pii/S2210670724006991.

Li, D., Yuan, J., & Kopp, R. E. (2020). Escalating global exposure to compound heat-humidity extremes with warming. *Environmental Research Letters*, *15*, Article 064003.

Liu, D., Zhou, R., Ma, Q., He, T., Fang, X., Xiao, L., Hu, Y., Li, J., Shao, L., & Gao, J. (2024). Spatio-temporal patterns and population exposure risks of urban heat island in megacity Shanghai, China. *Sustainable Cities and Society*, *108*, Article 105500.

Lyu, F., Zhou, L., Park, J., Baig, F., & Wang, S. (2024). Mapping dynamic human sentiments of heat exposure with location-based social media data. *International Journal of Geographical Information Science*, *38*, 1291–1314.

Mandvikar, K., Kumar, N., Supe, H., Singh, D., Gupta, A., Kumar, P., Meraj, G., Khan, I. D., Kouser, A., Pandey, S. K., et al. (2024). Evaluating heat health risk in Indian cities: geospatial and socio-ecological analysis. *World Development Sustainability*, *5*, Article 100180.

Ming, Y., Liu, Y., Liu, X., & Tian, Z. (2024). Demographic disparity in diurnal surface urban heat island exposure across local climate zones: A case study of Chongqing, China. *Science of the Total Environment*, *923*, Article 171203.

Mora, C., Dousset, B., Caldwell, I. R., Powell, F. E., Geronimo, R. C., Bielecki, C. R., Counsell, C. W., Dietrich, B. S., Johnston, E. T., Louis, L. V., et al. (2017). Global risk of deadly heat. *Nature Climate Change*, *7*, 501–506.

Probst, N., Bach, P. M., Cook, L. M., Maurer, M., & Leitão, J. P. (2022). Blue green systems for urban heat mitigation: mechanisms, effectiveness and research directions. *Blue-Green Systems*, *4*, 348–376.

Raj, S., Yerim, L., Yun, G. Y., & Santamouris, M. (2025). Contrasting urban heat disparities across income levels in Seoul and London. *Sustainable Cities and Society*, *121*, Article 106215.

Sharma, A., Dutta, P., Shah, P., Iyer, V., He, H., Sapkota, A., Gao, C., & Wang, Y. C. (2024). Characterizing the effects of extreme heat events on all-cause mortality: A case study in Ahmedabad city of India, 2002–2018. *Urban Climate*, *54*, Article 101832.

Singh, S., Mall, R., & Singh, N. (2021). Changing spatio-temporal trends of heat wave and severe heat wave events over India: An emerging health hazard. *International Journal of Climatology*, *41*, E1831–E1845.

Spector, J. T., Masuda, Y. J., Wolff, N. H., Calkins, M., & Seixas, N. (2019). Heat exposure and occupational injuries: review of the literature and implications. *Current Environmental Health Reports*, *6*, 286–296.

Stechemesser, A., & Wenz, L. (2023). Inequality in behavioural heat adaptation: an empirical study with mobility data from the transport system in New York City, NY, USA. *The Lancet Planetary Health*, *7*, e798–e808.

Suter, M. K., Miller, K. A., Anggraeni, I., Ebi, K. L., Game, E. T., Krenz, J., Masuda, Y. J., Sheppard, L., Wolff, N. H., & Spector, J. T. (2019). Association between work in deforested, compared to forested, areas and human heat strain: an experimental study in a rural tropical environment. *Environmental Research Letters*, *14*, Article 084012.

Tang, J., Zhao, P., Gong, Z., Zhao, H., Huang, F., Li, J., Chen, Z., Yu, L., & Chen, J. (2023). Resilience patterns of human mobility in response to extreme urban floods. *National Science Review*, *10*, Article nwad097.

Wang, C., Ren, Z., Guo, Y., Zhang, P., Hong, S., Ma, Z., Hong, W., & Wang, X. (2024). Assessing urban population exposure risk to extreme heat: Patterns, trends, and implications for climate resilience in China (2000–2020). *Sustainable Cities and Society*, *103*, Article 105260.

Wu, H., Jin, R., Liu, M., Nie, Z., Zhao, H., Yao, L., & Zhao, L. (2024). Investigating the potential of street trees in mitigating pedestrian thermal stress during heatwaves conditions: An empirical study in Guangzhou. *Building and Environment*, *265*, Article 111955. http://dx.doi.org/10.1016/j.buildenv.2024.111955, URL: https://www.sciencedirect.com/science/article/pii/S0360132324007972.

Wu, H., Zhang, G., Liu, Y., & Ming, Y. (2025). Addressing neighborhood effect averaging problem: Distinguishing mobility-based and residence-based heat exposure. *Building and Environment*, Article 113139.

Xiong, K., & He, B. J. (2024). Planning for heat-resilient educational precincts: Framework formulation, cooling infrastructure selection and walkable routes determination. *Sustainable Cities and Society*, *101*, Article 105183.

Yin, Y., Grundstein, A., Mishra, D. R., Ramaswamy, L., Tonekaboni, N. H., & Dowd, J. (2021). Dtex: A dynamic urban thermal exposure index based on human mobility patterns. *Environment International*, *155*, Article 106573.

Yin, Y., He, L., Wennberg, P. O., & Frankenberg, C. (2023). Unequal exposure to heatwaves in los angeles: Impact of uneven green spaces. *Science Advances*, *9*, Article eade8501. http://dx.doi.org/10.1126/sciadv.ade8501, URL: https://www.science.org/doi/abs/10.1126/sciadv.ade8501. arXiv:https://www.science.org/doi/pdf/10.1126/sciadv.ade8501.

Zhang, F., Li, Z., Li, N., & Fang, D. (2019). Assessment of urban human mobility perturbation under extreme weather events: A case study in Nanjing, China. *Sustainable Cities and Society*, *50*, Article 101671. http://dx.doi.org/10.1016/j.scs.2019.101671, URL: https://www.sciencedirect.com/science/article/pii/S221067071930719X.

Zhang, W., del Prado, M. N., Gauthier, V., & Milusheva, S. (2024). The netmob2024 dataset: Population density and od matrices from four lmic countries. URL: https://arxiv.org/abs/2410.00453. arXiv:2410.00453.

Zou, B., Fan, C., Wang, M., Li, J., Zhou, X., & Liao, Y. (2025). How do urban-rural and regional summer heat exposures evolve? A case study of 301 cities in China from 2000 to 2020. *Building and Environment*, *271*, Article 112584.